

Lanthanum anomalies provide constraints on macrofaunal predation at methane seeps

X. Wang, Z. Jia, J. Peckmann, S. Kiel, J.-A. Barrat, G. Bayon,
J. Li, L. Yin, T. Wei, Q. Liang, D. Feng

Supplementary Information

The Supplementary Information includes:

- Materials and Methods
- Tables S-1 to S-7
- Figures S-1 to S-7
- Supplementary Information References

Materials and Methods

Sample collection

Four metazoan taxa investigated in this study, including (1) the thiotrophy-dependent clam *Archivesica marissinica*, (2) the methanotrophy-dependent mussel *Gigantidas haimensis*, (3) the heterotrophic turrid gastropod *Phymorhynchus buccinoides*, and (4) the heterotrophic scale worm *Branchipolynoe pettiboneae* were collected with ROV *Haima* at approximately 1390 m water depth from the Haima methane seeps during a cruise in April 2023 (Fig. 1; Table S-1).

Dissection of macrofauna

The metazoans analysed in this study represent bivalves (one species of clams and mussels each), a gastropod (turrid), and a polychaete (scale worm), all of which possess distinct anatomical structures. To mitigate the risk of metal contamination, a ceramic knife was used for the dissection of metazoans. Clams and mussels were dissected into different types of tissue and hard parts, including adductors, feet, gills, visceral mass, mantle, and shells. Similarly, the turrid gastropod was dissected into columellar muscles, feet, gills, visceral mass, mantle, proboscis, and shells. In order to fulfill the criteria for subsequent geochemical analysis, scale worms were not subjected to dissection due to their limited size and weight (Fig. 1c). The dissected metazoans (and the undissected scale worms) were placed into centrifuge tubes and subjected to freeze-drying in preparation for subsequent analysis.

Rare earth element analysis

Based on the estimation of the rare earth element content in the subsamples, a certain mass of freeze-dried subsample was weighted. The weight of the polychaete as a whole, as well as the soft tissues of bivalves and gastropods, was



approximately 100 mg, while the weight of calcareous shells of bivalves and gastropods was around 200 mg. The samples were then transferred into an acid-washed 7 ml Teflon beaker and soaked in 1 ml concentrated HNO_3 . The lid of the Teflon beaker was initially kept open to prevent the accumulation of gas, before the beaker was placed on a heating plate (120 °C). After overnight reaction, the sample was evaporated and 1 ml concentrated HNO_3 was added again to dissolve the sample repeatedly. After two rounds of digestion and evaporation, the samples were subsequently dissolved in a 10 M H_2O_2 (drop by drop until no more bubbles evolved) and evaporated overnight. The samples were finally re-dissolved in a constant volume of 2 ml of 14 N HNO_3 (mother solution).

Due to the low concentration of rare earth elements in the samples and the high concentration of interfering matrix elements, the approach of Barrat *et al.* (2020) and Wang *et al.* (2020) was employed to eliminate the interfering elements (matrix) by passing the mother solution through a DGA resin. The new DGA resin was soaked and rinsed with 0.05 M HCl for 10 times before use. Finally, 1 ml of DGA resin was added to the chromatographic column tube. The detailed procedure was as follows:

Step	Purpose	Operation
1	Washing matrix elements within DGA resin	5 ml 0.05 N HCl × 10 times
2	Washing matrix elements within DGA resin, maintain acid balance of DGA resin	5 ml 14 N HNO_3 × 1 time
3	Elute all matrix elements (Ca, Mg, Sr) and Ba	3.5 ml 14 N HNO_3 × 2 times
4	Elute Fe	5 ml 2 N HNO_3 × 1 time
5	Collect the target elements (REE + Y)	5 ml 0.05 N HCl × 5 times

Note: Replace the DGA resin after repeating the above operations for 4 times.

The final step corresponds to the collection of target elements using 25 ml 0.05 N HCl (with a 100 ml plastic bottle, wash it with dilute acid and dry it in advance) followed by evaporation on the hotplate. The re-dissolved sample (in 2 ml 2 % HNO_3 , constant volume) with added internal standard was used for analyzing rare earth elements with ICP-MS. The analysis of a standard sample (CAL-S) verified the effectiveness and accuracy of the experimental procedure (Fig. S-1).

Internal standard: 20 ppb Rh

Instrument: ThermoFisher iCAPRQ ICP-MS

Standard samples: BHVO-2, W-2a and HPS standard solution (ICP-MS-68A-A-100 and ICP-MS-68A-B-100)

Analytical error: ≤5 %.

Trace element contents of the investigated metazoans are reported on dry matter basis, all rare earth elements were analysed at Hebei GEO University.

The calculation based on the Bayesian mixing model

In this study, we use an open-source R software package, MixSIAR, which is a flexible Bayesian tracer mixing model framework and a customizable tool that was developed on the basis of MixSIR (Moore and Semmens, 2008) and SIAR (Parnell *et al.*, 2010). Readers are recommended to look up the detailed procedures in the original research (Stock *et al.*, 2018).

To validate the Bayesian mixing model, we initially utilised the published carbon isotopes of the investigated metazoans (*i.e.* methanotrophy-dependent mussels, turrid gastropod *Phymorhynchus buccinoides*, and scale worm *Branchipolynoe pettiboneae*) from the Haima seeps. Additionally, we considered the carbon isotopes of dissolved organic carbon (DOC)



and particulate organic carbon (POC) in seawater at the Haima seeps (Table S-7). We employed MixSIAR to simulate the proportion of mussels serving as the carbon source for the turrid gastropod and the scale worm. It is important to acknowledge that the endmembers exhibit slight variation in the simulation of the turrid gastropod and the scale worm, owing to their distinct physiological behavior. The turrid gastropod exhibits a greater degree of omnivorous feeding behavior and has direct contact with sediment, resulting in the utilization of three distinct carbon isotope sources: mussel tissue, DOC, and POC. The scale worm predominantly inhabits methanotrophy-dependent mussels, exhibiting minimal susceptibility to sediments. Consequently, only two endmembers (*i.e.* mussel tissue and DOC), are considered relevant given their ecological niche. The results of the simulation indicate that the proportion of carbon derived from methanotrophy-dependent mussels in the turrid gastropod *Phymorhynchus buccinoides* accounts for approximately 51 % (Fig. S-6 a1 and a2), while in the scale worm *Branchipolynoe pettiboneae*, it accounts for approximately 88.4 % (Fig. S-7 a1 and a2).

Using the La enrichment in metazoan tissue and hard parts ($(La/Nd)_{sn}$) as endmember, the parameters are calculated as follows:

[1] Methanotrophy-dependent mussels:

$$[(La/Nd)_{sn}]_{whole} = \sum([(La/Nd)_{sn}]_F \times \text{mass}_F) / \text{total mass} \quad (\text{Eq. S-1})$$

where F represents adductors, feet, gills, visceral mass, mantle, and shells, respectively. This calculation method implicitly recognises that heterotrophic macrofauna do not exhibit a preference for specific tissues of mussels when preying on them, but rather consume all parts of the mussels in an indiscriminate manner.

[2] Turrid gastropod *Phymorhynchus buccinoides*:

As a heterotrophic omnivorous metazoan, the turrid gastropod has the ability to acquire La from various sources such as seawater, sediments, and mussels. Therefore, the potential sources of La anomalies in their visceral mass are:

$$[(La/Nd)_{sn}]_{visceral\ mass} = F1 \times [(La/Nd)_{sn}]_{sw} + F2 \times [(La/Nd)_{sn}]_{SED} + F3 \times [(La/Nd)_{sn}]_{whole} \quad (\text{Eq. S-2})$$

where F1, F2 and F3 represent the proportion of $(La/Nd)_{sn}$ from seawater, sediments, and mussels, respectively.

[3] Scale worm *Branchipolynoe pettiboneae*:

Scale worms are unlikely to receive significant contributions of La from sediments. Therefore, the potential sources of La are as follows:

$$[(La/Nd)_{sn}] = F1 \times [(La/Nd)_{sn}]_{sw} + F2 \times [(La/Nd)_{sn}]_{whole} \quad (\text{Eq. S-3})$$

where F1 and F2 are the proportion of $(La/Nd)_{sn}$ from seawater and mussels, respectively.

[4] Seawater and sediment:

$(La/Nd)_{sn}$ values of seawater and sediment of Haima seeps are taken from the literature (Table S-7).

Using the Bayesian mixing model, it can be calculated that the proportion of La derived from methanotrophy-dependent mussels – and consequently the proportion of mussel tissue among the different food sources – is approximately 50.4 % for the turrid gastropod *Phymorhynchus buccinoides* (Fig. S-6 b1 and b2) and approximately 87.9 % for the scale worm *Branchipolynoe pettiboneae* (Fig. S-7 b1 and b2).



Supplementary Tables (Tables S-1 to S-7)

Table S-1 Sample information.

Macrofauna	Species	Trophic mode	Sample ID	Length	Width	Height	Adductors	Feet	Gills	Visceral mass	Mantle	Shells	
				(cm)			g (dry weight)						
Bathymodioline mussel	<i>Gigantidas haimaensis</i>	Methanotroph	GH1	11.1	5.3	2.2	0.0847	0.1779	0.4519	0.4883	0.5095	5.55	
			GH2	11.5	5.4	3.1	0.2776	0.2552	1.4385	1.3075	2.5028	5.75	
			GH3	10.2	5.0	2.2	0.2112	0.3681	1.1157	0.6457	0.982	5.1	
Pliocardiine clam	<i>Archivesica marissinica</i>	Thiotroph	AM1	15.1	6.9	2.5	1.3814	2.2925	6.6673	3.3503	2.2691	—	
			AM2	14.7	6.3	2.5	1.1313	1.9154	5.3934	2.2625	1.7688	—	
			AM3	15.6	6.7	2.5	1.2684	2.6816	4.9503	3.5415	2.4636	—	
				g (as a whole, dry weight)									
Scale worm	<i>Branchipolynoe pettiboneae</i>	Heterotroph	BP1	0.0927									
			BP2	0.1522									
			BP3	0.1345									
			BP4	0.1678									
			BP5	0.1422									
			BP6	0.1625									
			BP7	0.1672									
			BP8	0.1535									
			BP9	0.1166									
			BP10	0.0970									
			BP11	0.1434									
			BP12	0.1111									
			BP13	0.1299									
				Columellar muscles		Feet	Gills	Visceral mass	Mantle	Proboscis	Shells		
Turrid gastropod	<i>Phymorhynchus buccinoides</i>	Heterotroph	PB1										
			PB2	—									



			PB3														
			PB4														
			PB5														

Sampling site: Haima seeps in the northwestern South China Sea
 Sampling date: April 2023
 Water depth: ~ 1390 m
 “—” means no data

Table S-2 ΣREE + Y abundances (in ng/g) of *Archivesica marissinica*.

Sample ID	La	Ce	Pr	Nd	Sm	Eu	Gd	Tb	Dy	Y	Ho	Er	Tm	Yb	Lu	La/La*	Ce/Ce*
Adductors																	
AM1-A	85.59	38.27	11.82	51.12	10.74	2.81	16.21	1.95	9.12	104.86	1.57	3.30	0.37	2.00	0.27	2.28	0.44
AM2-A	162.52	178.72	28.42	112.79	19.89	2.69	12.65	0.51	—	18.73	—	0.78	0.06	0.41	0.07	1.52	0.78
AM3-A	569.10	1068.96	129.70	511.37	100.38	19.67	97.63	9.76	—	326.00	1.12	3.49	0.22	2.08	0.24	1.15	1.02
Feet																	
AM1-F	106.35	54.01	14.05	58.64	11.90	2.99	15.02	1.94	9.32	134.19	1.54	3.22	0.40	2.04	0.29	2.22	0.50
AM2-F	212.65	73.65	28.81	124.82	25.86	6.82	37.90	4.83	24.78	289.81	4.89	11.97	1.33	7.21	1.07	2.33	0.35
AM3-F	202.45	156.21	32.28	132.87	26.96	6.51	33.57	4.33	21.58	242.54	4.25	10.67	1.22	6.69	1.00	1.79	0.62
Gills																	
AM1-G	237.95	51.28	25.89	96.06	13.37	2.73	12.47	0.58	—	51.33	0.33	1.27	0.12	0.87	0.13	2.13	0.23
AM2-G	33.79	33.89	3.80	13.23	2.22	0.46	2.57	0.25	1.02	6.55	0.18	0.48	0.06	0.39	0.06	1.82	0.97
AM3-G	606.31	260.67	82.25	343.02	55.18	6.38	31.72	1.15	—	47.01	—	1.47	—	0.27	0.02	2.16	0.41
Visceral																	
AM1-V	174.38	44.94	20.96	90.99	19.03	4.92	26.07	3.28	16.05	212.84	3.00	6.95	0.80	4.47	0.68	2.64	0.29
AM2-V	239.66	186.06	37.25	156.76	33.55	8.17	39.96	4.44	15.79	278.18	3.80	13.14	1.54	10.55	1.93	1.92	0.66
AM3-V	449.64	432.93	77.70	313.12	62.72	14.29	70.72	8.39	30.01	405.01	3.31	5.46	0.65	3.55	0.46	1.58	0.70
Mantle																	
AM1-M	311.21	99.57	40.04	169.66	35.14	9.07	47.39	6.23	32.69	376.02	6.68	16.63	1.88	9.91	1.53	2.35	0.33
AM2-M	787.65	1186.41	163.85	659.64	133.45	28.47	137.56	18.38	91.32	638.95	17.08	44.19	5.43	31.53	4.53	1.31	0.91
AM3-M	606.37	800.29	122.70	515.17	102.44	22.02	120.64	12.47	43.32	488.05	5.88	13.46	1.48	8.92	1.14	1.47	0.86
Shells																	



AM1-S	4.99	8.88	1.05	4.24	0.94	0.22	1.03	0.14	0.70	4.29	0.13	0.36	0.05	0.31	0.05	1.32	1.08
AM2-S	40.26	65.45	6.31	27.63	5.48	1.26	6.16	0.75	3.74	25.00	0.71	1.86	0.23	1.40	0.21	2.06	1.42
AM3-S	107.22	168.31	16.78	73.69	13.20	3.04	17.07	1.99	10.18	77.19	2.09	5.90	0.72	4.50	0.68	2.08	1.38

“—” means no data

Table S-3 Σ REE + Y abundances (in ng/g) of *Gigantidas haimensis*.

Sample ID	La	Ce	Pr	Nd	Sm	Eu	Gd	Tb	Dy	Y	Ho	Er	Tm	Yb	Lu	La/La*	Ce/Ce*
Adductors																	
GH1-A	64.38	49.10	4.00	12.72	2.41	0.47	2.26	0.19	0.69	9.15	0.13	0.37	0.05	0.37	0.06	2.73	1.22
GH2-A	74.30	62.26	4.95	13.82	1.49	0.27	1.93	0.13	0.31	12.59	0.04	0.14	0.01	0.08	0.01	1.97	1.10
GH3-A	99.68	134.44	17.07	66.85	13.72	2.79	13.46	1.57	4.89	42.79	0.52	1.06	0.11	0.71	0.10	1.51	0.96
Feet																	
GH1-F	84.85	64.11	4.83	13.62	2.40	0.36	1.84	0.13	0.54	11.05	0.11	0.34	0.05	0.32	0.05	2.35	1.17
GH2-F	87.39	73.64	5.90	16.25	2.31	0.57	3.84	0.38	1.85	23.57	0.39	1.11	0.14	0.87	0.13	1.89	1.07
GH3-F	48.30	43.19	4.59	15.20	2.18	0.48	2.33	0.28	1.16	29.66	0.18	0.50	0.07	0.45	0.08	1.94	0.97
Gills																	
GH1-G	1243.65	363.74	38.58	71.95	11.11	1.87	10.98	0.99	2.68	38.07	0.25	0.49	0.06	0.33	0.04	1.89	0.55
GH2-G	832.58	328.98	34.64	67.08	10.09	1.72	11.51	1.11	4.86	32.87	0.87	2.16	0.26	1.50	0.21	1.52	0.58
GH3-G	1654.08	411.73	50.55	83.91	11.51	2.06	19.61	1.14	2.70	30.64	0.26	0.66	0.05	0.35	0.04	1.52	0.42
Visceral																	
GH1-V	476.61	256.04	20.66	48.66	10.44	1.61	9.33	0.65	1.21	32.30	0.17	0.53	0.06	0.48	0.08	2.16	0.91
GH2-V	192.54	169.81	13.77	37.40	5.18	1.10	6.48	0.73	3.60	28.12	0.70	1.76	0.22	1.23	0.18	1.74	1.05
GH3-V	133.36	133.26	14.72	50.75	10.46	1.91	9.49	0.62	1.81	28.92	0.37	1.23	0.15	1.11	0.20	1.81	0.98
Mantle																	
GH1-M	170.98	131.47	10.17	28.65	4.32	0.76	4.54	0.35	1.15	15.24	0.19	0.51	0.06	0.34	0.05	2.25	1.14
GH2-M	715.76	162.17	82.69	367.13	73.50	18.04	86.44	—	—	463.17	—	1.70	—	1.27	0.08	2.87	0.27
GH3-M	114.50	82.68	9.10	29.44	5.47	1.16	5.68	0.63	2.93	17.38	0.55	1.52	0.19	1.17	0.17	2.21	0.92
Shells																	
GH1-S	52.57	21.00	1.89	5.32	0.93	0.22	1.47	0.14	0.44	12.30	0.06	0.13	0.02	0.10	0.02	3.71	0.98
GH2-S	71.44	36.27	2.99	8.13	1.23	0.44	2.22	0.22	1.06	14.16	0.22	0.60	0.08	0.50	0.08	2.98	1.03
GH3-S	53.54	38.06	4.05	12.45	1.89	0.41	2.90	0.30	1.45	18.26	0.28	0.76	0.10	0.63	0.10	2.10	0.90

“—” means no data



Table S-4 ΣREE + Y abundances (in ng/g) of *Phymorhynchus buccinoides*.

Sample ID	La	Ce	Pr	Nd	Sm	Eu	Gd	Tb	Dy	Y	Ho	Er	Tm	Yb	Lu	La/La*	Ce/Ce*
Columellar																	
PB1-CM	48.10	42.50	6.44	24.26	5.05	0.93	4.41	0.41	0.97	19.42	0.11	0.26	0.03	0.20	0.03	1.79	0.78
PB2-CM	40.15	19.14	3.14	10.75	2.69	0.42	2.38	0.24	0.91	6.88	0.14	0.33	0.04	0.26	0.04	2.53	0.65
PB3-CM	51.87	40.86	5.93	22.22	8.06	1.09	5.91	0.71	3.51	26.69	0.68	1.84	0.24	1.62	0.26	2.07	0.81
PB4-CM	25.98	25.58	3.84	15.06	3.58	0.65	3.27	0.27	0.67	14.77	0.10	0.29	0.04	0.26	0.04	1.76	0.82
PB5-CM	24.23	17.53	3.00	11.69	3.02	0.43	1.97	0.13	0.59	10.73	0.19	0.71	0.08	0.55	0.09	2.07	0.71
Feet																	
PB1-F	457.50	895.60	107.17	415.30	83.30	16.56	80.55	9.32	22.64	278.84	1.66	3.84	0.32	2.45	0.29	1.08	1.01
PB2-F	80.91	139.04	18.40	72.42	15.67	3.01	15.93	1.83	6.39	48.30	0.70	1.40	0.16	0.96	0.11	1.15	0.93
PB3-F	55.53	88.37	10.90	41.64	9.42	1.82	7.95	1.07	5.08	33.92	0.88	2.12	0.28	1.65	0.24	1.25	0.97
PB4-F	37.08	53.16	6.72	26.14	5.59	1.02	4.72	0.46	1.14	20.41	0.12	0.29	0.03	0.23	0.03	1.40	0.96
PB5-F	67.29	102.00	12.18	46.54	13.01	2.02	9.35	1.21	5.64	42.23	0.97	2.41	0.30	1.83	0.26	1.36	1.00
Gills																	
PB1-G	99.09	107.36	17.05	70.18	16.95	3.40	18.01	2.30	11.17	85.32	2.04	5.13	0.66	4.35	0.70	1.66	0.81
PB2-G	333.77	590.77	71.58	274.22	57.38	11.28	53.63	6.51	21.47	171.22	2.32	5.14	0.58	3.83	0.52	1.15	0.99
PB3-G	355.18	245.85	56.93	238.35	47.20	7.69	30.88	—	—	78.98	—	1.27	0.04	0.53	0.05	1.84	0.57
PB4-G	176.93	109.84	13.42	43.21	5.87	0.63	4.78	0.20	—	5.01	—	0.24	0.01	0.07	0.01	2.30	0.82
PB5-G	122.68	55.26	9.04	34.81	9.59	1.48	6.37	0.45	1.15	—	0.18	0.53	0.07	0.36	0.05	3.39	0.74
Visceral mass																	
PB1-V	193.91	124.15	16.74	56.72	6.77	—	4.28	0.22	0.28	1.80	0.07	—	0.04	0.24	0.04	2.24	0.79
PB2-V	348.66	83.47	22.80	80.27	18.09	3.72	22.35	2.48	11.44	124.85	2.07	4.90	0.57	3.40	0.50	3.19	0.40
PB3-V	355.58	228.16	24.38	73.50	12.09	2.48	16.58	1.55	6.15	40.72	0.95	2.15	0.25	1.50	0.20	2.23	0.88
PB4-V	411.81	237.28	29.41	86.81	15.60	3.05	19.82	1.94	8.08	60.71	1.20	2.64	0.33	2.04	0.27	2.06	0.74
PB5-V	175.51	120.73	13.91	46.36	9.70	1.53	8.06	0.39	0.34	—	0.04	—	0.02	0.18	0.02	2.36	0.91
Mantle																	
PB1-M	48.96	62.05	8.71	34.84	7.72	1.51	7.21	0.62	0.91	—	0.08	0.33	0.03	0.25	0.04	1.51	0.89
PB2-M	793.36	1271.11	176.41	688.56	135.03	27.85	125.57	17.30	84.86	535.21	14.27	33.53	4.53	26.33	3.51	1.15	0.88
PB3-M	109.45	178.12	22.76	88.33	19.13	3.62	17.74	2.27	9.02	66.90	1.15	2.24	0.28	1.62	0.20	1.22	0.95
PB4-M	60.87	84.64	10.76	42.28	9.47	1.77	8.87	1.07	4.32	36.99	0.57	1.12	0.14	0.84	0.11	1.47	0.97



PB5-M	41.22	60.24	9.34	36.90	8.62	1.41	6.92	0.83	4.02	22.53	0.85	1.70	0.21	1.31	0.19	1.16	0.80
Proboscis																	
PB1-P	32.63	35.59	5.37	22.18	6.05	1.45	6.95	1.38	16.41	75.58	4.55	11.29	1.35	7.57	1.19	1.74	0.86
PB2-P	19.91	20.85	3.18	12.24	2.90	0.54	2.82	0.33	1.49	9.00	0.26	0.66	0.08	0.52	0.08	1.57	0.79
PB3-P	28.33	23.77	3.58	13.16	3.72	0.58	2.76	0.37	1.85	13.88	0.35	0.92	0.11	0.74	0.12	1.80	0.76
PB4-P	27.29	35.24	5.23	21.77	6.32	1.38	5.74	0.85	5.76	54.71	1.51	4.90	0.59	3.59	0.56	1.52	0.88
PB5-P	24.64	25.20	3.66	13.91	4.22	0.58	2.83	0.30	0.89	—	0.10	0.21	0.02	0.15	0.02	1.64	0.82
Shells																	
PB1-S	114.53	119.09	17.28	72.37	14.11	3.42	15.62	2.11	10.43	95.08	1.76	3.85	0.50	2.84	0.40	1.96	0.90
PB2-S	82.72	88.89	12.70	52.64	11.77	2.73	14.24	1.85	9.10	60.32	1.66	4.30	0.54	3.37	0.49	1.89	0.91
PB3-S	114.60	100.61	20.41	92.40	19.56	5.01	26.98	3.36	15.05	169.42	2.38	5.30	0.65	3.90	0.51	1.94	0.70
PB4-S	124.96	108.12	17.60	74.79	14.37	3.31	15.75	1.78	6.80	86.62	1.00	2.23	0.28	1.68	0.25	2.16	0.82
PB5-S	133.76	144.93	21.75	94.79	19.50	4.70	24.51	3.17	16.46	111.90	3.21	8.25	0.96	5.82	0.83	1.97	0.91

“—” means no data

Table S-5 ΣREE + Y abundances (in ng/g) of *Branchipolynoe pettiboneae*.

Sample	La	Ce	Pr	Nd	Sm	Eu	Gd	Tb	Dy	Y	Ho	Er	Tm	Yb	Lu	La/La*	Ce/Ce*
Whole																	
BP1	239.10	93.21	14.61	60.98	14.17	3.41	20.11	2.46	12.62	113.43	2.66	7.18	0.92	5.60	0.91	4.80	0.83
BP2	536.16	144.29	18.45	76.71	18.02	4.41	23.95	3.05	13.30	167.94	1.90	3.53	0.48	2.64	0.36	8.46	1.02
BP3	416.00	49.71	6.17	20.00	3.73	0.39	2.40	0.14	0.43	2.32	0.09	0.32	0.03	0.20	0.03	11.95	0.82
BP4	314.94	143.91	15.63	59.67	9.90	1.09	7.09	0.47	1.26	12.50	0.28	1.12	0.12	0.74	0.12	4.95	1.10
BP5	328.73	66.97	8.01	30.53	6.93	1.67	8.89	0.99	2.85	58.05	0.39	1.10	0.13	0.85	0.14	10.04	1.00
BP6	344.19	79.98	10.82	40.90	7.31	0.60	3.88	0.18	0.28	4.58	0.08	0.37	0.03	0.19	0.03	7.65	0.87
BP7	125.79	34.69	4.54	17.90	2.01	0.08	1.07	0.08	0.27	—	0.09	0.39	0.05	0.31	0.06	7.27	0.94
BP8	514.47	62.59	7.47	26.17	3.00	0.24	2.98	0.34	1.58	8.18	0.26	0.68	0.10	0.60	0.11	14.23	0.92
BP9	123.73	36.40	5.43	22.73	5.33	1.39	7.33	0.96	3.59	62.36	0.53	1.23	0.17	1.02	0.17	6.74	0.88
BP10	249.54	210.93	24.75	95.94	20.61	4.27	21.17	1.89	3.16	88.73	0.35	1.13	0.12	0.82	0.12	2.55	1.03
BP11	318.65	43.70	5.86	21.54	5.01	1.19	5.37	0.23	0.39	23.10	0.07	0.28	0.04	0.28	0.05	12.37	0.86
BP12	539.66	369.55	42.22	159.13	33.01	6.54	32.89	4.01	15.24	123.03	2.25	5.89	0.73	4.77	0.77	3.06	1.03
BP13	156.00	115.14	12.73	49.21	9.98	1.71	7.49	0.30	0.32	11.55	0.06	0.38	0.03	0.25	0.04	3.08	1.09

“—” means no data



Table S-6 ΣREE + Y abundances (in ng/g) of standard CAL-S in this and previous studies.

Sample ID	La	Ce	Pr	Nd	Sm	Eu	Gd	Tb	Dy	Y	Ho	Er	Tm	Yb	Lu	La/La*	Ce/Ce*
CAL-S																	
This study	603.33	231.24	68.26	286.57	50.64	12.60	74.32	11.48	77.44	1406.37	19.67	60.27	8.11	47.25	7.22	2.62	0.44
Potts <i>et al.</i> , 2000	787.00	333.00	90.00	357.00	64.00	16.00	93.00	14.00	100.00	1944.00	26.00	81.00		68.00	11.00	2.32	0.46
Le Goff <i>et al.</i> , 2019	793.00	302.00	87.10	359.00	62.40	15.50	91.60	13.70	98.30	2065.00	26.00	81.00		66.30	10.16	2.61	0.45
Wang <i>et al.</i> , 2020	806	313	89.2	363	63.7	15.9	92.3	13.9	99.6	2177	26.3	82		67.1	10.3	2.52	0.45
Barrat <i>et al.</i> , 2020	806	313	89.2	363	63.7	15.85	92.3	13.9	100	2177	26.33	82		67.1	10.31	2.52	0.45
Barrat <i>et al.</i> , 2022	759	310	89.2	369	64.3	16.07	93.3	14	100	2072	26.29	81.9		66.3	10.18	2.45	0.45

Table S-7 Parameters for the Bayesian mixed model.

Sample	$\delta^{13}\text{C}$	Reference	Sample	$\delta^{13}\text{C}$	Reference	
<i>Branchipolynoe pettiboneae</i>	-58.9	Feng <i>et al.</i> , 2015	Mussel	-76.4	Feng <i>et al.</i> , 2015	
	-50.6	Ke <i>et al.</i> , 2022		-75.2		
<i>Phymorhynchus buccinoides</i>	-46.9			-73.4		
<i>Phymorhynchus</i> sp.	-48.2			-77.6		
DOC	-22.3	Ding <i>et al.</i> , 2022		-76.4		
	-22.4			-72.8		
POC	-28.5	Ke <i>et al.</i> , 2022		-74.3		
	-29.7			-69.3		
	-29.5			-67.7		
	-30.6			-70.1		
	-28.2			-69.6		
	-39.3			-65.2		
	-32.4			-71.2		
	-27.2			-68.3		



Mussel	-27.2		-64.7	
	-49.8		-70.7	
	-52.7	Ke <i>et al.</i> , 2022	-68.2	
	-60.7		-66.2	
	-61.9		-71.5	
	-59.8		-68.0	
	-59.3		-66.0	
	-63.7		-70.3	
	-61.7		-69.0	
	-59.8		-66.1	
	-60.8		-72.9	
	-61.8		-72.4	
	-62.8		-68.5	
	-62.9		-74.9	
	-59.3		-73.5	
	-61.5		-69.6	
	-59.3		-70.0	
	-61.0		-68.1	
	-59.0		-66.2	
	-60.0		-71.1	
	-61.3		-70.4	
	-59.3		-66.5	
	-59.9		-63.2	Zhao <i>et al.</i> , 2020
	-58.9		-66.6	
	-64.8		-68.7	
	-61.1			
	-58.9	Sample	(La/Nd) _{sn}	Reference
	-61.5	Seawater (1488 m, SCS)	1.20	Alibo and Nozaki, 2000
	-63.0	Sediment (Haima)	0.97	Wang <i>et al.</i> , 2020



-60.6
-61.8
-60.5
-61.4
-56.3
-57.2
-55.1
-56.2
-56.5
-52.3
-55.2
-58.7
-53.4



Supplementary Figures (Figures S-1 to S-7)

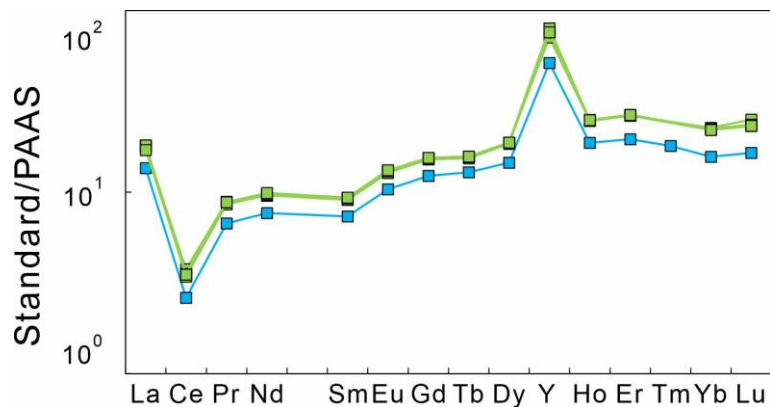


Figure S-1 REE+Y patterns normalised to Post Archaean Australian Shale (PAAS, Pourmand *et al.*, 2012) for the CAL-S standard (blue) analysed during the course of the study. See Table S-6 for the reference values from five other studies (green).

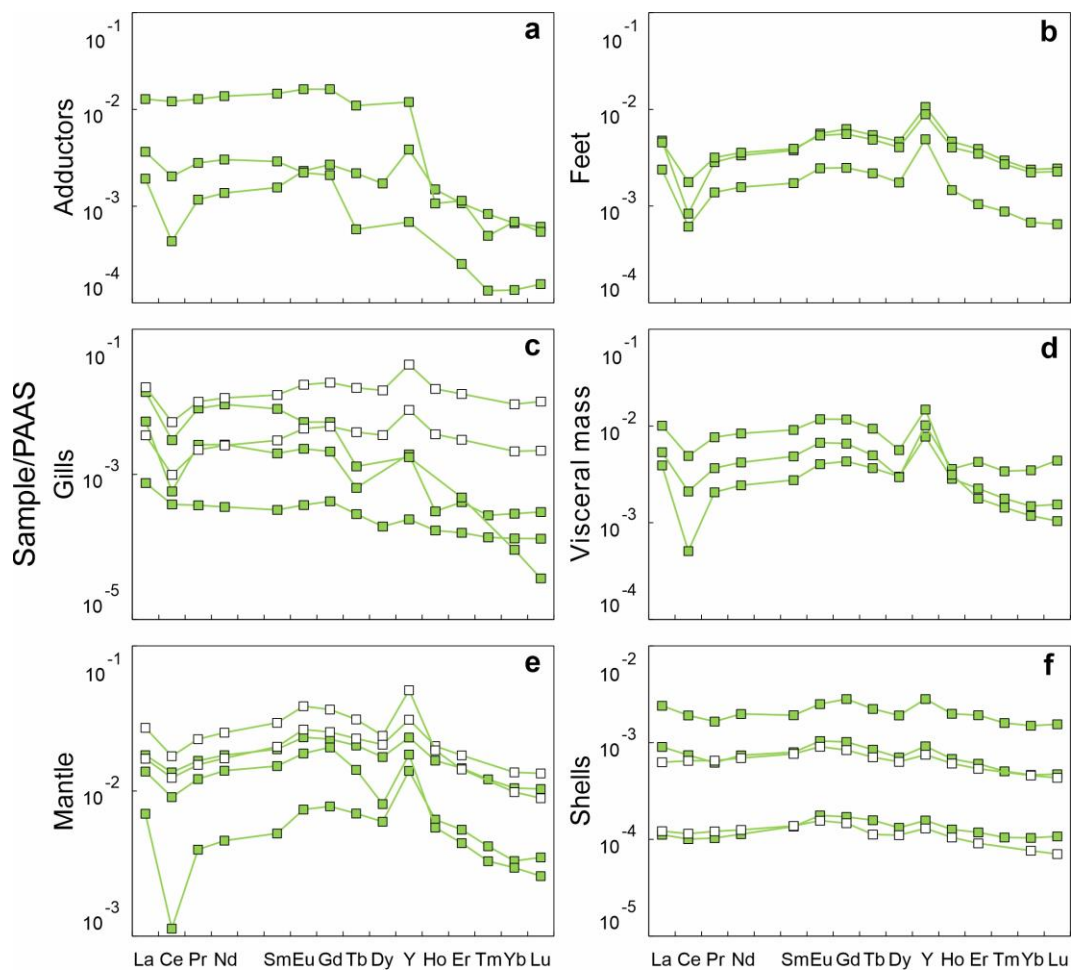


Figure S-2 REE + Y patterns normalised to PAAS (Pourmand *et al.*, 2012) for the clam *Archivesica marissinica* with thiotrophic symbionts from Haima seeps. **(a)** Adductors; **(b)** feet; **(c)** gills; **(d)** visceral mass; **(e)** mantle; **(f)** shells. Data represented by hollow squares are from Wang *et al.* (2020).



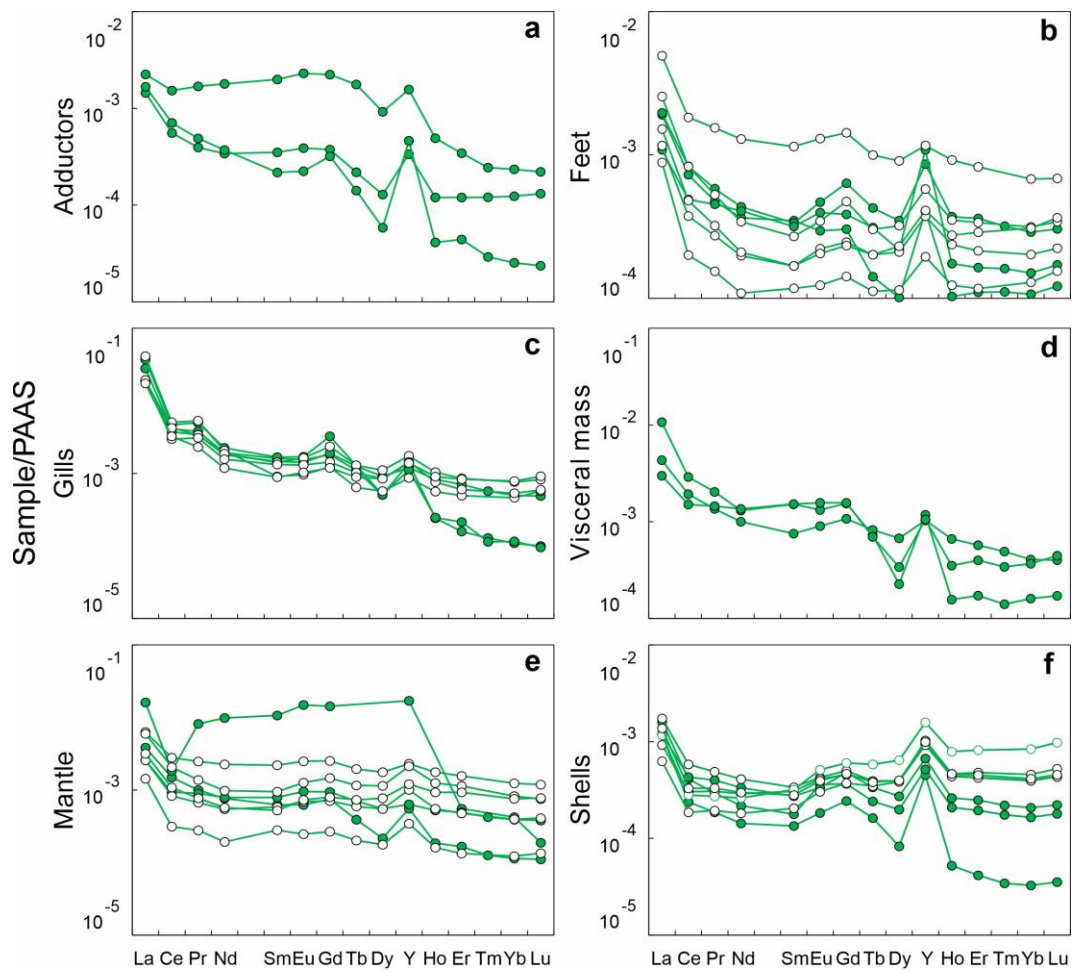


Figure S-3 REE + Y patterns normalised to PAAS (Pourmand *et al.*, 2012) for the mussel *Gigantidas haimaensis* with methanotrophic symbionts from Haima seeps. **(a)** Adductors; **(b)** feet; **(c)** gills; **(d)** visceral mass; **(e)** mantle; **(f)** shells. Data represented by hollow circles are from Wang *et al.* (2020).



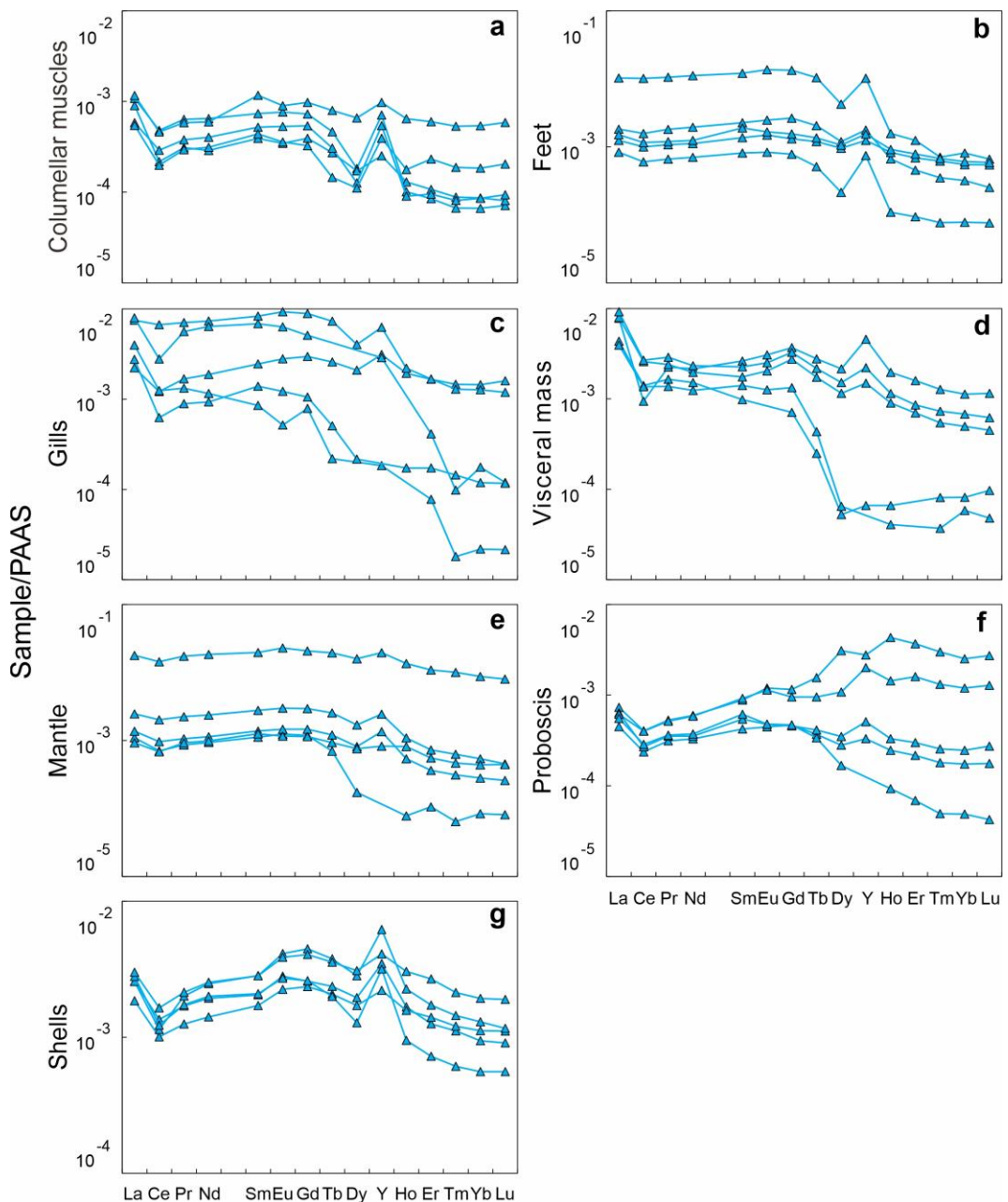


Figure S-4 REE + Y patterns normalised to PAAS (Pourmand *et al.*, 2012) for the heterotrophic turrid gastropod *Phymorhynchus buccinoides* from Haima seeps. **(a)** Columellar muscles; **(b)** feet; **(c)** gills; **(d)** visceral mass; **(e)** mantle; **(f)** proboscis; **(g)** shells.



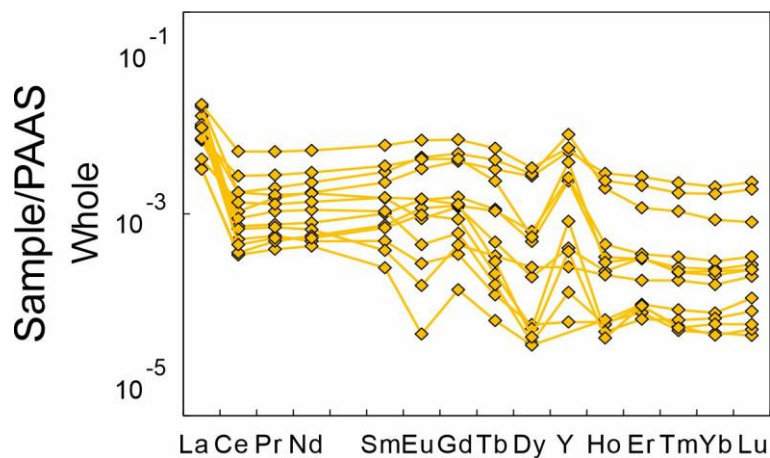


Figure S-5 REE + Y patterns normalised to PAAS (Pourmand *et al.*, 2012) for the heterotrophic scale worm *Branchipolynoe pettiboneae* (as a whole) from Haima seeps.



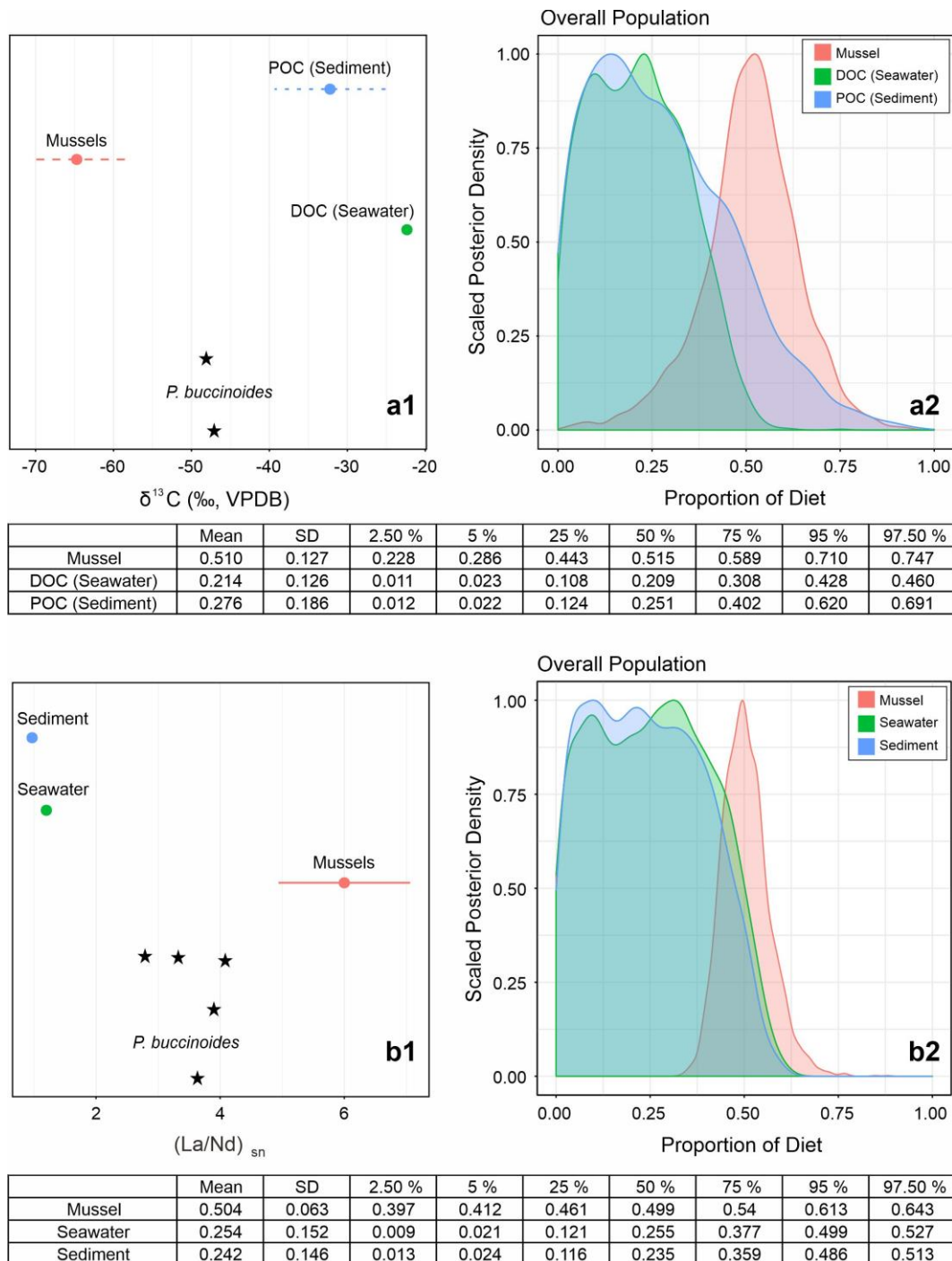


Figure S-6 Calculation of food sources of the heterotrophic turrid gastropod *Phymorhynchus buccinoides* by a Bayesian mixing model. **(a1-a2)** Based on carbon isotope composition; **(b1-b2)** Based on (La/Nd)_{sn} ratios.



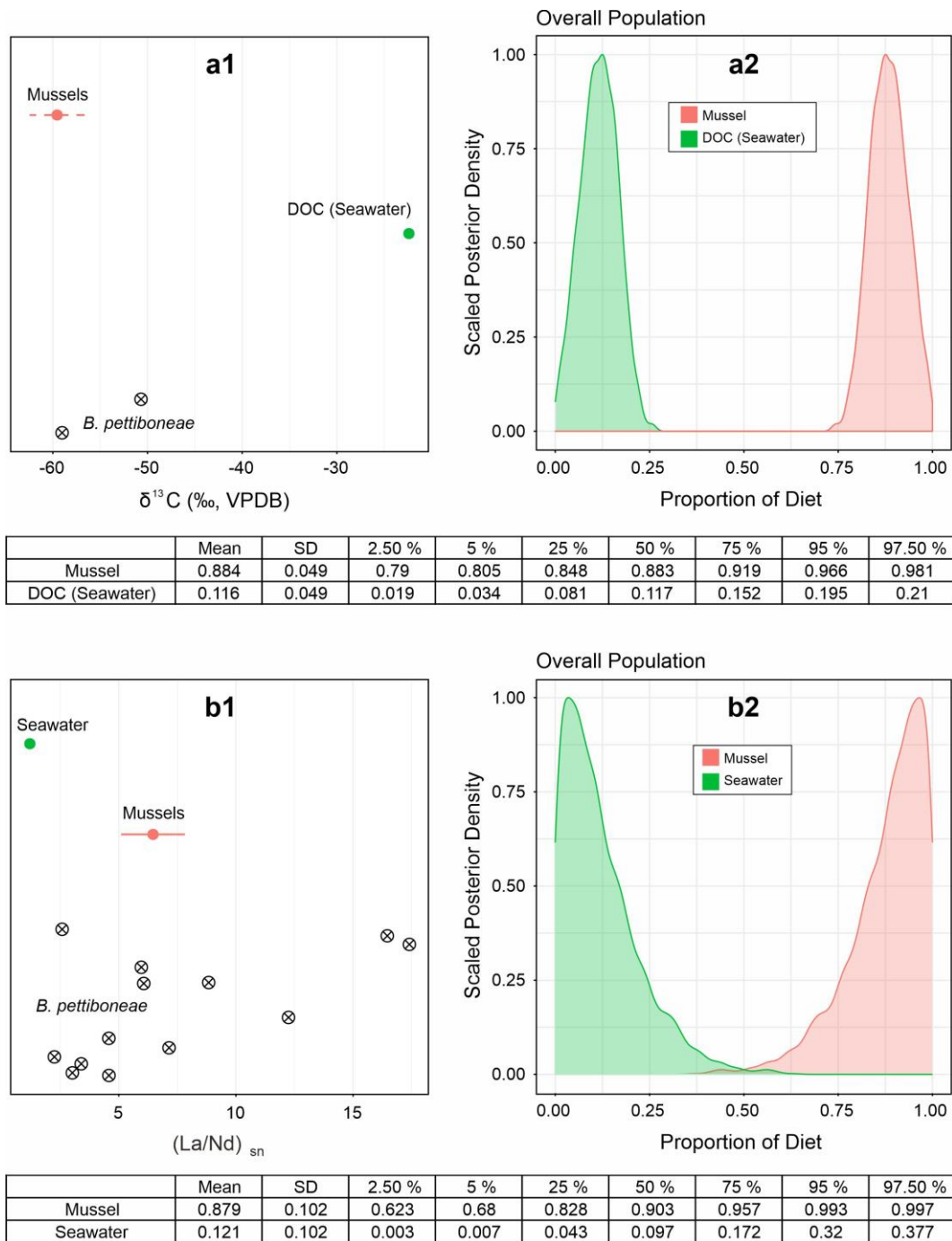


Figure S-7 Calculation of food sources of the heterotrophic scale worm *Branchipolynoe pettiboneae* by a Bayesian mixing model. **(a1-a2)** Based on carbon isotope composition; **(b1-b2)** Based on $(\text{La}/\text{Nd})_{\text{sn}}$ ratios.



Supplementary Information References

- Alibo, D.S., Nozaki, Y. (2000) Dissolved rare earth elements in the South China Sea: geochemical characterization of the water masses. *Journal of Geophysical Research* 105, 28771–28783. <https://doi.org/10.1029/1999JC000283>
- Barrat, J.-A., Bayon, G., Wang, X., Le Goff, S., Rouget, M.L., Gueguen, B., Salem, D.B. (2020) A new chemical separation procedure for the determination of rare earth elements and yttrium abundances in carbonates by ICP-MS. *Talanta* 219, 121244. <https://doi.org/10.1016/j.talanta.2020.121244>
- Barrat, J.-A., Chauvaud, L., Olivier, F., Poitevin, P., Bayon, G., Salem, D.B. (2022) Rare earth elements and yttrium in suspension-feeding bivalves (dog cockle, *Glycymeris glycymeris* L.): Accumulation, vital effects and pollution. *Geochimica et Cosmochimica Acta* 339, 12–21. <https://doi.org/10.1016/j.gca.2022.10.033>
- Ding, L., Shan, S., Luo, C., Wang, X. (2022) Distribution and microbial degradation of dissolved organic carbon in the northern South China Sea. *Frontiers in Marine Science* 9, 973694. <https://doi.org/10.3389/fmars.2022.973694>
- Feng, D., Cheng, M., Kiel, S., Qiu, J.-W., Yang, Q., Zhou, H., Peng, Y., Chen, D. (2015) Using *Bathymodiolus* tissue stable carbon, nitrogen and sulfur isotopes to infer biogeochemical process at a cold seep in the South China Sea. *Deep-Sea Research I* 104, 52–59. <https://doi.org/10.1016/j.dsr.2015.06.011>
- Ke, Z., Li, R., Chen, Y., Chen, D., Chen, Z., Lian, X., Tan, Y. (2022) A preliminary study of macrofaunal communities and their carbon and nitrogen stable isotopes in the Haima cold seeps, South China Sea. *Deep-Sea Research I* 184, 103774. <https://doi.org/10.1016/j.dsr.2022.103774>
- Le Goff, S., Barrat, J.-A., Chauvaud, L., Paulet, Y.M., Gueguen, B., Salem, B.D. (2019) Compound-specific recording of gadolinium pollution in coastal waters by great scallops. *Scientific Reports* 9, 8015. <https://doi.org/10.1038/s41598-019-44539-y>
- Moore, J.W., Semmens, B.X. (2008) Incorporating uncertainty and prior information into stable isotope mixing models. *Ecology Letters* 11, 470–480. <https://doi.org/10.1111/j.1461-0248.2008.01163.x>
- Parnell, A.C., Inger, R., Bearhop, S., Jackson, A.L. (2010) Source partitioning using stable isotopes: coping with too much variation. *PLoS One* 5, e9672. <https://doi.org/10.1371/journal.pone.0009672>
- Potts, P.J., Thompson, M., Kane, J.S., Webb, P.C., Carignan, J. (2000) GEOPT6 - an international proficiency test for analytical geochemistry laboratories - report on round 6 (OU-3: Nanhoron microgranite) and 6A (CAL-S: CRPG limestone). International Association of Geoanalysts. <https://www.geoanalyst.org/wp-content/uploads/2017/10/GeoPT06-6AReport.pdf>
- Pourmand, A., Dauphas, N., Ireland, T.J. (2012) A novel extraction chromatography and MC-ICP-MS technique for rapid analysis of REE, Sc and Y: Revising CI-chondrite and Post-Archean Australian Shale (PAAS) abundances. *Chemical Geology* 291, 38–54. <https://doi.org/10.1016/j.chemgeo.2011.08.011>
- Stock, B.C., Jackson, A.L., Ward, E.J., Parnell, A.C., Phillips, D.L., Semmens, B.X. (2018) Analyzing mixing systems using a new generation of Bayesian tracer mixing models. *PeerJ* 6, e5096. <https://doi.org/10.7717/peerj.5096>
- Wang, X., Barrat, J.A., Bayon, G., Chauvaud, L., Feng, D. (2020) Lanthanum anomalies as fingerprints of methanotrophy. *Geochemical Perspectives Letters* 14, 26–30. <https://doi.org/10.7185/geochemlet.2019>
- Wang, X., Guan, H., Qiu, J.-W., Xu, T., Peckmann, J., Chen, D., Feng, D. (2022) Macro-ecology of cold seeps in the South China Sea. *Geosystems and Geoenvironment* 1, 100081. <https://doi.org/10.1016/j.geogeo.2022.100081>
- Zhao, Y., Xu, T., Law, Y.S., Feng, D., Li, N., Xin, R., Wang, H., Ji, F., Zhou, H., Qiu, J.-W. (2020) Ecological characterization of cold-seep epifauna in the South China Sea. *Deep-Sea Research I* 163, 103361. <https://doi.org/10.1016/j.dsr.2020.103361>

